

First-principles design of excitonic insulators: A review

Hongwei Qu(曲宏伟), Haitao Liu(刘海涛), and Yuanchang Li(李元昌)
Citatio: Chin. Phys. B, 2025, 34 (**9**): 097101. DOI: 10.1088/1674-1056/ade073
http://cpb.iphy.ac.cn; http://iopscience.iop.org/cpb

What follows is a list of articles you may be interested in

Anionic electron dimensionality and monolayer ferromagnetism in Y-Co electrides

Lu Zheng(郑璐), Zimeng Lv(吕梓萌), Xiaochen Huang(黄小琛), Zhuangfei Zhang(张壮飞), Chao Fang(房超), Yuewen Zhang(张跃文), Qianqian Wang(王倩倩), Liangchao Chen(陈良超), Xiaopeng Jia(贾晓鹏), Biao Wan(万彪), and Huiyang Gou(缑慧阳)
Chin. Phys. B, 2025, 34 (**9**): 097105. DOI: 10.1088/1674-1056/adf82f

First-principles calculations on strain tunable hyperfine Stark shift of shallow donors in Si

Zi-Kai Zhou(周子凯) and Jun Kang(康俊)
Chin. Phys. B, 2025, 34 (**8**): 087102. DOI: 10.1088/1674-1056/addeba

Interacting Dirac semi-metal state in nonsymmorphic Kondo-lattice compound $CeAgSb_2$

Da-Liang Guo(郭达良), and Huan Li(黎欢)
Chin. Phys. B, 2025, 34 (**6**): 067102. DOI: 10.1088/1674-1056/adc6f6

Predicted stable two-dimensional semiconductor TiOS materials with promising photocatalytic properties: First-principles calculations

Pan Zhang(张攀), Shihai Fu(付世海), Chunying Pu(濮春英), Xin Tang(唐鑫), and Dawei Zhou(周大伟)
Chin. Phys. B, 2025, 34 (**5**): 057103. DOI: 10.1088/1674-1056/adb687

Strain-modulated superconductivity of monolayer Tc_2B_2

Zhengtao Liu(刘正涛), Zihan Zhang(张子涵), Hao Song(宋昊), Tian Cui(崔田), and Defang Duan(段德芳)
Chin. Phys. B, 2025, 34 (**4**): 047104. DOI: 10.1088/1674-1056/adb94d

---

TOPICAL REVIEW — Exciton physics: Fundamentals, materials and devices

First-principles design of excitonic insulators: A review

Hongwei Qu(曲宏伟)[1], Haitao Liu(刘海涛)[2,3], and Yuanchang Li(李元昌)[1,†]

[1] *Key Laboratory of Advanced Optoelectronic Quantum Architecture and Measurement (MOE), and School of Interdisciplinary Science, Beijing Institute of Technology, Beijing* 100081, *China*

[2] *Institute of Applied Physics and Computational Mathematics, Beijing* 100088, *China*

[3] *National Key Laboratory of Computational Physics, Beijing* 100088, *China*

(Received 25 April 2025; revised manuscript received 30 May 2025; accepted manuscript online 4 June 2025)

The excitonic insulator (EI) is a more than 60-year-old theoretical proposal that is still elusive. It is a purely quantum phenomenon involving the spontaneous generation of excitons in quantum mechanics and the spontaneous condensation of excitons in quantum statistics. At this point, the excitons represent the ground state rather than the conventional excited state. Thus, the scarcity of candidate materials is a key factor contributing to the lack of recognized EI to date. In this review, we begin with the birth of EI, presenting the current state of the field and the main challenges it faces. We then focus on recent advances in the discovery and design of EIs based on the first-principles Bethe–Salpeter scheme, in particular the dark-exciton rule guided screening of materials. It not only opens up new avenues for realizing excitonic instability in direct-gap and wide-gap semiconductors, but also leads to the discovery of novel quantum states of matter such as half-EIs and spin-triplet EIs. Finally, we will look ahead to possible research pathways leading to the first recognized EI, both theoretically and computationally.

Keywords: excitonic insulator, Bose condensation, first-principles, Bethe–Salpeter equation (BSE)

PACS: 71.35.Lk, 73.22.–f, 81.05.Hd, 11.10.St

DOI: 10.1088/1674-1056/ade073 **CSTR:** 32038.14.CPB.ade073

1. Introduction

The past two decades have witnessed tremendous achievements in first-principles design of novel quantum materials, especially topological materials. In 2017, Varsano *et al.*[1] employed the first-principles Bethe–Salpeter scheme to predict that carbon nanotubes are intrinsic excitonic insulators (EIs). In 2018, Jiang *et al.*[2] proposed a dark-exciton rule for the occurrence of excitonic instability, which provides a useful guide for finding and designing EIs. Since then, researchers have successfully predicted a wide variety of EIs through this approach, including band-engineered EIs, topological EIs, and magnetic EIs. The rise of two-dimensional materials has rekindled the 60-year-old EI mystery, leading to advances in materials, theory, and experiment. In this review, we will focus on advances in first-principles design of EI candidates. For other aspects, see the reviews, e.g., Refs. [3–6].

1.1. The birth of EI

In the 1930s, Frenkel[7,8] and Peierls[9] conceptualised excitons as fundamental excitations of solids, which are electron-hole pairs bound together by Coulomb attraction. At length scales larger than the exciton radius, they can be regarded as bosons and are therefore capable of Bose–Einstein condensation.[10] For the first 30 years, excitons were studied as excited states. It was not until 1961 that Mott[11] first suggested that in semimetals with low carrier concentrations, excitons might spontaneously arise and open an energy gap, leading to a metal-insulator phase transition. Two years later, Knox proposed a condition for spontaneous exciton generation (excitonic instability), i.e., the exciton binding energy E_b exceeds its single-electron excitation gap E_g.[12] With further developments by Keldysh and Kopaev,[13] and DesCloizeaux,[14] Jérome *et al.*[15] proposed that, for semimetals with a small overlapping of valence and conduction bands or for semiconductors with a small bandgap, there may exist a new state of matter at low temperatures in which excitons are spontaneously generated and condense to a BCS-like state. They named this state of matter the EI.

Later, Halperin and Rice[16] gave a more precise definition of an EI. Here we quote their original words: "Let us focus our attention on the crystal at 0 K, in the semiconducting region with E_g close to E_b. For $E_g > E_b$, no excitons are present in the ground state of the crystal, and the nondistorted state is stable. For $E_g < E_b$, excitons are present. In this region, treating the crystal in a Hartree–Fock approximation is roughly equivalent to treating the excitons as a weakly repulsive Bose gas. Excitons form until the repulsive potential cancels the negative energy $(E_g - E_b)$ associated with the creation of a single exciton. Furthermore, and most important, the excitons present will form a Bose condensate in the exciton state

†Corresponding author. E-mail: yuancli@bit.edu.cn

© 2025 Chinese Physical Society and IOP Publishing Ltd. All rights, including for text and data mining, AI training, and similar technologies, are reserved.

of minimum energy, namely the state with wave vector $\boldsymbol{w}$."

The EI is another macroscopic quantum state analogous to superconductors and superfluids, essentially originating from many-body interactions between electrons. It involves the spontaneous generation of excitons in quantum mechanics and spontaneous condensation in quantum statistics. At this point, the exciton is the ground state of the system, not the excited state.[16,17] Now the single-electron picture breaks down, and the system displays bosonic physics. The study of EI contributes to a deeper understanding of many-body interactions in condensed-matter physics and helps to shed light on the superconductivity/superfluidity mechanism. Whether EI correlates with some kind of supertransport phenomenon could provide further evidence for the study of the relationship between Bose condensation and superfluidity.[15–21] Since exciton binding is typically much stronger than Cooper pairs, EIs have a greater potential to maintain quantum correlations at or above room temperature, thus providing a new material platform for quantum information technology.

1.2. Developments and bottlenecks

Despite entering a new era, the EI remains elusive.[6] The lack of recognized EI to date is mainly due to the following two limitations.

(i) Scarcity of material platforms. Excitons were originally introduced to explain the photoexcitation behavior of semiconductors, and hence they are used to describe an excited state rather than a ground state. In other words, spontaneous generation of excitons is very rare. Known EI candidates, both those predicted in theory and those with experimental tests, can be broadly classified into three categories. The first category is semimetals with small overlapping between valence and conduction bands, or semiconductors with small bandgaps, which were proposed at the inception of EI. This list includes transition-metal dichalcogenides,[22–29] Ta_2NiSe_5,[21,30–32] $Ta_2Pd_3Te_5$,[33–37] and some other nanostructures.[38–40] Among them, $TiSe_2$ and Ta_2NiSe_5 are representative star materials that have received intensive attention. They have the advantage of the presence of easily experimentally recognisable phase transition signals, but the disadvantage of being accompanied by structural distortions. Experimentally, there is a lack of robust means to distinguish whether the phase transition is exciton-driven or simply originated from the Jahn–Teller effect.[24,31]

The second category is the electron–hole bilayer structure, which is traditionally realized using semiconductor quantum wells.[41,42] The emergence of two-dimensional van der Waals heterojunctions in recent years has rapidly made this paradigm a hot topic in EI research.[43–48] The spatial separation of electrons and holes allows for longer lifetimes of interlayer excitons, and non-equilibrium exciton condensation at ~ 100 K has been experimentally demonstrated.[49] However, the so-called "exciton" here is in fact an electron–hole composite fermion pair, which is insufficient to explain all the features of "real" excitons. Despite some inherent shortcomings of this scheme in fully understanding EI, such as spontaneous symmetry breaking, it does provide a wealth of useful insights. In this review, our focus is on excitonic instability in intrinsic materials.

The third category is theoretically suggested wide-gap semiconductors in recent years, mainly in low-dimensional systems.[2,50–58] It shows that excitonic instabilities can occur even in strongly correlated semiconductors with $E_g > 3$ eV.[50,51] The wide gap naturally suppresses the Jahn–Teller distortions, thus avoiding the intrusion of structural mechanisms. The drawback, however, is that the insulator–insulator phase transition in this case loses an easily recognizable signal of the kind seen experimentally in a metal–insulator transition. This raises a new question of how to distinguish between a many-body gap and a single-electron gap.[55]

(ii) Lack of a deterministic identification method for experiments. As defined in Subsection 1.1, the EI is a theoretical mechanism that is not defined by observable phenomena. This contrasts with superconductors, which are founded on two well-defined experimental phenomena: zero resistance and the Meissner effect. A more practical challenge is that most contemporary exciton detection techniques rely on observing the evolution of systems under external energy injection.[59] By contrast, the EI is precisely the ground state and its appearance does not require an input of energy. Although for a given material, spontaneous condensation of excitons can be inferred by comparing the crystal structure, characteristics of the frontier state, and optical properties of the high-temperature and low-temperature phases,[22,30,41,60] at this stage of knowledge the presence of all these signals can only indicate that the exciton mechanism may be one of the possibilities, and it is not possible to completely rule out other competing mechanisms, such as the Jahn–Teller effect, the Mott transition, and other mechanisms. This is the fundamental reason why EIs are still full of controversy after more than half a century of research. On the other hand, some researchers have attempted to determine spontaneous exciton condensation by measuring the superflow phenomenon, but the charge-neutrality of excitons makes electrical measurements extremely challenging. In addition, it is theoretically controversial whether EIs are capable of generating a form of superfluidity since they have a diagonal long-range order.[17–20]

1.3. First-principles Bethe–Salpeter scheme

As defined by Halperin and Rice,[16] an EI is simply a substance for which $E_g < E_b$ at 0 K. The first-principles Bethe–Salpeter scheme is able to quantify these two quanti-

ties, which makes it a powerful tool for finding and designing EIs.

To obtain E_g using density functional theory (DFT)-based methods, one needs to solve the equation

$$\left(-\frac{1}{2}\nabla^2 + v_{\rm nu}(\boldsymbol{r}) + v_{\rm H}([n];\boldsymbol{r}) + \Theta\right)\phi_i(\boldsymbol{r}) = \varepsilon_i\phi_i(\boldsymbol{r}),$$
$$[n] = \sum_i^N |\phi_i(\boldsymbol{r})^2|. \quad (1)$$

Here the first three terms refer to the kinetic energy, the nuclear potential, and the Hartree potential, which remain formally consistent regardless of the calculation method. The difference between the different methods is reflected in the approximation to the fourth term Θ. For standard DFT, it is given by local or semi-local exchange–correlation potentials. However, such approximations systematically underestimate E_g of semiconductors and insulators by more than 30%.[61–63] To overcome this problem, Θ in GW employs a non-local and energy-dependent potential (self-energy). However, compared with DFT, GW calculations greatly increase the computational cost, so a balance between computational accuracy and efficiency must be considered in practice. At present, in most cases, a single-shot G_0W_0 calculation is used instead of a fully self-consistent GW.[51,61]

To obtain E_b, one needs to solve the Bethe–Salpeter equation (BSE), which reduces to an eigenvalue problem of the Hamiltonian[64]

$$H_{vckv'c'k'} = (\varepsilon_{ck} - \varepsilon_{vk})\delta_{vv'}\delta_{cc'}\delta_{kk'} + (f_{ck} - f_{vk})(2V_{vckv'c'k'} - W_{vckv'c'k'}). \quad (2)$$

The first term arises from the single-electron eigenvalues in Eq. (1). The second term is the BSE kernel, where $W_{vckv'c'k'}$ and $V_{vckv'c'k'}$ represent an attractive screened electron–hole interaction and a repulsive Coulomb exchange interaction, respectively. Sometimes, a "scissor operator" is employed to address the bandgap problem. This method is relatively less computationally demanding and in good agreement with experiment.[53,65] Since different computational methods usually change the band shape only slightly, applying a scissor operator Δ to rigidly shift the conduction band away from the valence band by Δ yields a new single-electron band, which is then taken as a new input for solving the BSE. Notably, this not only changes the first term of the Hamiltonian (2) from $\varepsilon_{ck} - \varepsilon_{vk}$ to $\varepsilon_{ck} - \varepsilon_{vk} + \Delta$, but also leads to a modification of $W_{vckv'c'k'}$, which in turn changes E_b.[53] It is noteworthy that the scissor operator is only a compromise relative to a self-consistent GW computation, and its reliability needs to be carefully examined.

2. First-principles design of EIs

2.1. Dark-exciton rule

For a material to be an EI, it must satisfy $E_b > E_g$. Therefore, the larger E_b is, the more favourable it is for EI formation. According to the hydrogen atom model, it can be seen that a decrease in dimension leads to an enhancement of E_b and a reduction of the exciton radius. For example, the ground state energy of a two-dimensional hydrogen atom is four times that of a three-dimensional one, and is even divergent in one dimension.[57] It is evident that low-dimensional materials offer more opportunities for realizing EI.

However, simply increasing E_b is not enough, as E_b and E_g tend to show a subtle correlation. As illustrated in Fig. 1(a), decreasing E_g makes electronic excitation less difficult, thus favouring exciton formation; at the same time, this leads to an increase in the system screening, which in turn inhibits the exciton formation. A zero-gap system is intrinsically more favourable for EI formation, since any finite electron–hole interaction leads to the opening of an exciton gap. However, things are not so straightforward.

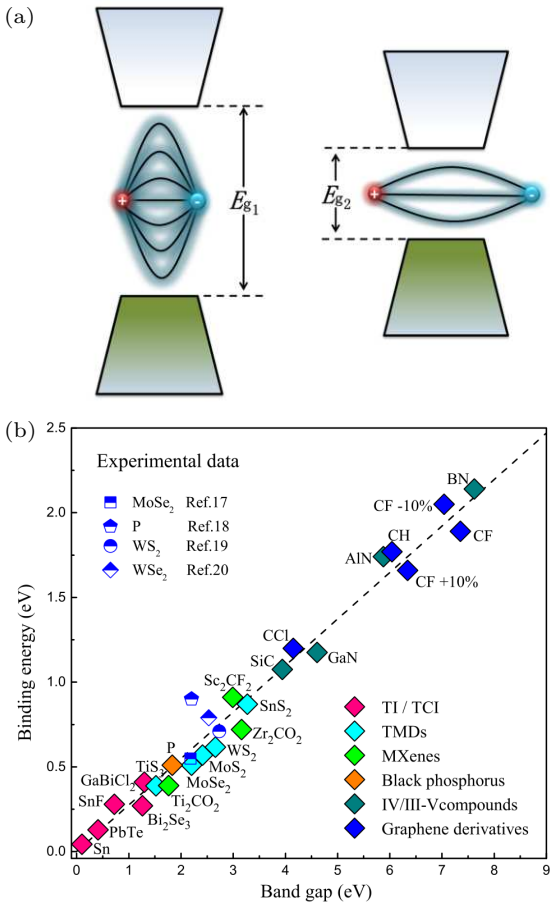


Fig. 1. (a) A diagrammatic illustration of the correlation between E_g and E_b. A larger E_g corresponds to weaker screening, stronger exciton binding, a smaller radius, and thus a higher E_b. Conversely, a smaller E_g results in stronger screening, weaker exciton binding, a larger radius, and a lower E_b. (b) The linear 1/4 scaling relationship between E_b and E_g in two-dimensional materials. Adapted from Ref. [67].

Let us consider the polarizability ε of a system, calculated

as

$$\varepsilon = A\sum_{c,v}\int_{\boldsymbol{k}} \frac{|\langle u_{c,\boldsymbol{k}}|\nabla_{\boldsymbol{k}}|u_{v,\boldsymbol{k}}\rangle|^2}{E_{c,\boldsymbol{k}}-E_{v,\boldsymbol{k}}}\mathrm{d}\boldsymbol{k}, \tag{3}$$

where $u_{c,\boldsymbol{k}}$ and $u_{v,\boldsymbol{k}}$ are the periodic parts of the conduction and valence band Bloch states, respectively, $\boldsymbol{k}$ is integrated over the first Brillouin zone, and A is a dimension-dependent coefficient. By definition, the minimum denominator $E_{c,\boldsymbol{k}} - E_{v,\boldsymbol{k}}$ is the band gap E_g of a direct-gap material. As $E_\mathrm{g} \to 0$, Eq. (3) shows that ε diverges, which implies E_b vanishes rather than remains finite. Therefore, simply reducing E_g or enhancing E_b does not guarantee the emergence of an EI.[2] Even in two-dimensional semiconductors, Choi *et al.*[66] identified a quantitative relationship between E_b and E_g, later refined by Jiang *et al.*[67] to a linear 1/4 scaling, as shown in Fig. 1(b). However, when the band-edge states $u^{\mathrm{cbm}}_{c,\boldsymbol{k}}$ and $u^{\mathrm{vbm}}_{v,\boldsymbol{k}}$ make the numerator $\langle u^{\mathrm{cbm}}_{c,\boldsymbol{k}}|\nabla_{\boldsymbol{k}}|u^{\mathrm{vbm}}_{v,\boldsymbol{k}}\rangle$ identically zero, the variation of E_g has no effect on Eq. (3). In this case, ε remains invariant, implying that E_b is independent of E_g and both are mutually decoupled. Consequently, if E_g can be tuned close to zero, an EI will inevitably emerge.

Within the first-principles BSE framework, $\langle u_{c,\boldsymbol{k}}|\nabla_{\boldsymbol{k}}|u_{v,\boldsymbol{k}}\rangle$ represents the dipole moment. A finite dipole moment leads to optically active (bright) excitons, whereas a vanishing one yields optically inactive (dark) excitons. We thus define $\langle u^{\mathrm{cbm}}_{c,\boldsymbol{k}}|\nabla_{\boldsymbol{k}}|u^{\mathrm{vbm}}_{v,\boldsymbol{k}}\rangle = 0$ as the *dark-exciton rule*, which states that transitions between the band-edge states are optically forbidden. This is physically intuitive: dark excitons are not dissipated by radiative recombination and therefore have longer lifetimes. The dark-exciton rule explains why EIs are often observed in indirect-gap semiconductors/semimetals and electron–hole bilayers. The former is due to momentum conservation and the latter due to spatial separation of carriers, both yielding $\langle u^{\mathrm{cbm}}_{c,\boldsymbol{k}}|\nabla_{\boldsymbol{k}}|u^{\mathrm{vbm}}_{v,\boldsymbol{k}}\rangle = 0$. By contrast, the rule also suggests that excitonic instability may occur in direct-gap systems.[2] Unlike the indirect-gap case, where electrons and holes occupy different $\boldsymbol{k}$-points, in direct-gap systems they reside at the same point in the Brillouin zone, fundamentally suppressing Jahn–Teller distortions such as those found in $1T$-$TiSe_2$.

2.2. EIs via band engineering

There are several possible routes to realize the condition $\langle u^{\mathrm{cbm}}_{c,\boldsymbol{k}}|\nabla_{\boldsymbol{k}}|u^{\mathrm{vbm}}_{v,\boldsymbol{k}}\rangle = 0$. One example is when the band-edge states share the same parity, making transitions between them dipole-forbidden.[2] Two-dimensional III–V semiconductors in the double-layer honeycomb structure, such as AlSb, exhibit frontier states of identical odd parity.[53,68–70] First-principles BSE calculations indeed reveal a negative transition energy E_t (defined as $E_\mathrm{t} = E_\mathrm{g} - E_\mathrm{b}$), signaling the possibility of an EI. Notably, such a two-dimensional AlSb structure has recently been fabricated on graphene-covered SiC(0001), where a band gap of 0.93 eV was measured.[71]

Equation (3) further highlights that EIs can be engineered by tuning E_g and/or E_b through band engineering. Such modulation can be achieved via strain, isoelectronic doping, or external electric/magnetic fields, among other means.[2,52,72,73] Figure 2(a) shows the calculated dependence of E_g and the two-dimensional polarizability $\alpha_{2\mathrm{D}}$ on strain for double-layer honeycomb GaAs. The results indicate that E_g varies linearly with strain, whereas $\alpha_{2\mathrm{D}}$ remains nearly constant in the positive-E_g region and diverges sharply once the system becomes metallic. This demonstrates that E_g is independent of dielectric screening. Importantly, the strain-independent $\alpha_{2\mathrm{D}}$ does not follow solely from the dark-exciton rule but is instead a consequence of the specific band structure of GaAs.[2]

BSE calculations confirm that E_b is indeed decoupled from E_g, as illustrated in Fig. 2(b). Regardless of the modulation method, the E_b and E_g curves always intersect at some point. Thus, although present first-principles methods cannot yet predict E_g with high accuracy, the excitonic instability identified here is robust and independent of the computational approach.

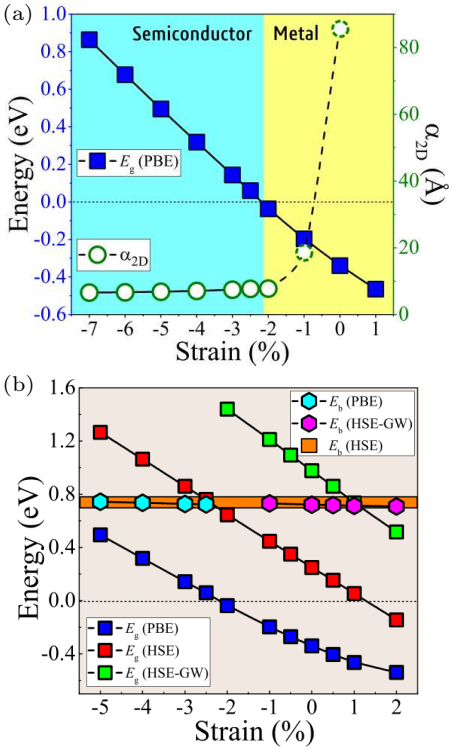


Fig. 2. (a) Strain dependence of the band gap E_g and the two-dimensional polarizability $\alpha_{2\mathrm{D}}$ for double-layer honeycomb GaAs. (b) Strain dependence of E_g and the exciton binding energy E_b obtained from different computational methods. Adapted from Ref. [2].

Similar physics occurs in monolayer TiS_3. Unlike double-layer GaAs, its band gap E_g decreases under compressive strain, and a band reordering occurs near -2%.[2] Fortunately, the bands near the Fermi energy share the same parity, so the band reordering does not alter the relevant physics.

Compressive strain can also be effectively implemented via isoelectronic substitution with larger-radius atoms, generating so-called chemical pressure. This has been demonstrated experimentally by alloying Se into monolayer TiS_3.[74] Calculations show that when Se replaces the middle S atoms, E_g decreases to roughly half that of pristine TiS_3, whereas E_b remains nearly unchanged.[52] Consequently, in TiS_2Se, $E_g < E_b$, indicating that Se doping drives a transition from a band insulator to an EI.

An external electric field can likewise induce an excitonic phase transition.[55] As shown in Fig. 3(a), the band gap E_g of a one-dimensional molecular wire $MnCp_\infty$ decreases significantly with increasing transverse electric field. This behavior arises because the valence and conduction band frontier orbitals respond differently to the field (see the top two rows of Fig. 3(b)). The valence-band maximum is primarily derived from Mn d-orbitals and is less sensitive to the field, whereas the conduction-band minimum originates mainly from π orbitals formed by the Cp ligands' p-electrons. Under the field, delocalized π electrons accumulate on one side, shifting the conduction band downward and reducing E_g. When the field reaches 0.2 V/Å, the band gap decreases by approximately 0.5 eV.

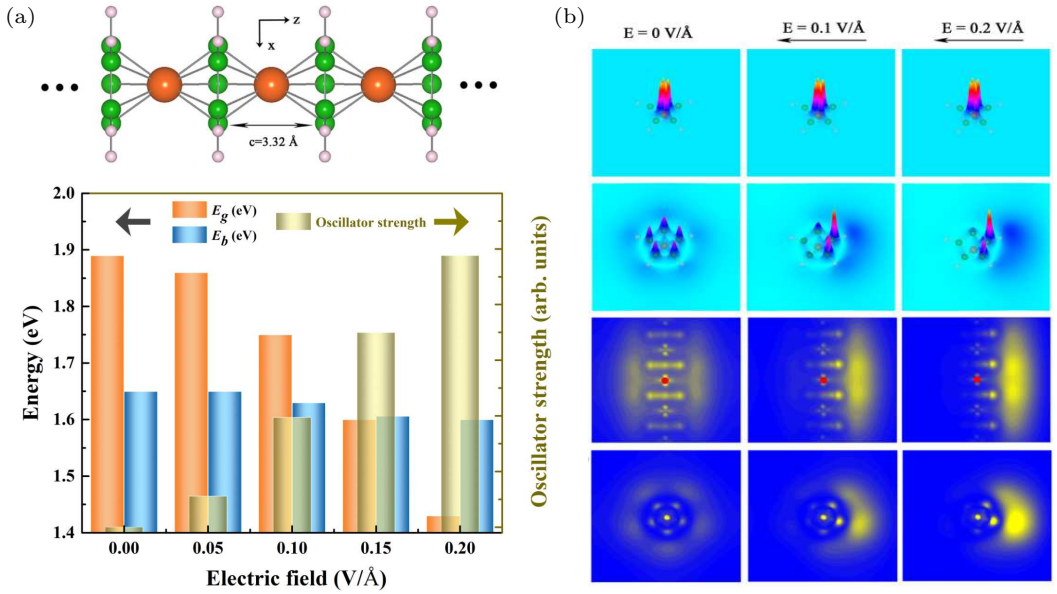


Fig. 3. (a) Top row: Geometric structure of the one-dimensional molecular wire $MnCp_\infty$. Bottom row: Band gap E_g, exciton binding energy E_b, and oscillator strength of the lowest-energy exciton as a function of applied electric field. On either side of the critical field near 0.15 V/Å, the relative magnitudes of E_g and E_b invert, indicating a phase transition between the band insulator and the EI. The oscillator strengths in the EI phase calculated from the current first-principles BSE have no physical significance; differences appear only near the phase transition. (b) Top two rows: Illustration of E_g narrowing due to the giant Stark effect. The valence-band maximum originates from localized Mn d-orbitals and is minimally affected by the electric field (first row), whereas the conduction-band minimum originates from delocalized π-orbitals, which shift downward under the field as electrons accumulate on one side of the two C atoms (second row), reducing the system's potential energy and the band gap. Bottom two rows: Evolution of the real-space wave function of the lowest-energy exciton under a transverse electric field. Red dots indicate hole positions fixed at central Mn atoms. Adapted from Ref. [55].

In the absence of an applied electric field, the lowest-energy exciton of $MnCp_\infty$ is located at 0.24 eV and is dark, resulting in a decoupling of E_b and E_g. This decoupling is confirmed by calculations: as shown in Fig. 3(a), E_b is nearly insensitive to the electric field, decreasing only from 1.65 eV to 1.60 eV as the field increases from 0 V/Å to 0.2 V/Å. This 0.05 eV change is an order of magnitude smaller than the corresponding variation in E_g. The differing responses of E_b and E_g to the electric field lead to a decrease of E_t with increasing field. When the field reaches approximately 0.15 V/Å, E_t becomes negative, signaling spontaneous exciton generation and the onset of the EI phase.

An additional interesting feature of electric-field modulation is its ability to alter the optical activity of excitons.[55,56] This effect could provide new opportunities for detecting EIs and for designing optical devices, which will be discussed later.

2.3. Topological EIs

Topological EIs represent a distinctive class of topological materials in which excitonic instability emerges. They offer potential opportunities at the intersection of topological insulators and excitonic insulators.[41,75–82] From the topological insulator perspective, first, spontaneous exciton condensation increases the bulk gap, potentially enabling higher operating temperatures. Second, the bulk gap in topological EIs originates from excitons rather than spin-orbit coupling (SOC), broadening the range of candidate materials beyond heavy-element systems. Third, exciton condensation is governed by the system's overall screening, making it less sensitive to certain defects. From the EI perspective, while the charge neu-

trality of excitons prevents direct electrical conduction, topological edge states provide a pathway for transport. Moreover, topological EIs could host exotic fully supertransport behavior, featuring bulk exciton superfluidity and dissipation-free edge transport.

This raises the question: which materials could intrinsically realize topological EIs? Consider, without loss of generality, a centrosymmetric system with a band gap. To be a topological insulator, it would require parity inversion, so its band-edge states should have opposite parity. In contrast, the dark-exciton rule indicates that excitonic instability is favored when band-edge states share the same parity, allowing E_g and E_b to be decoupled. This apparent contradiction is illustrated in Fig. 4(a): should the band-edge states of topological EIs have opposite or identical parity? This dilemma is analogous to spin frustration and is sometimes referred to as parity frustration.[80]

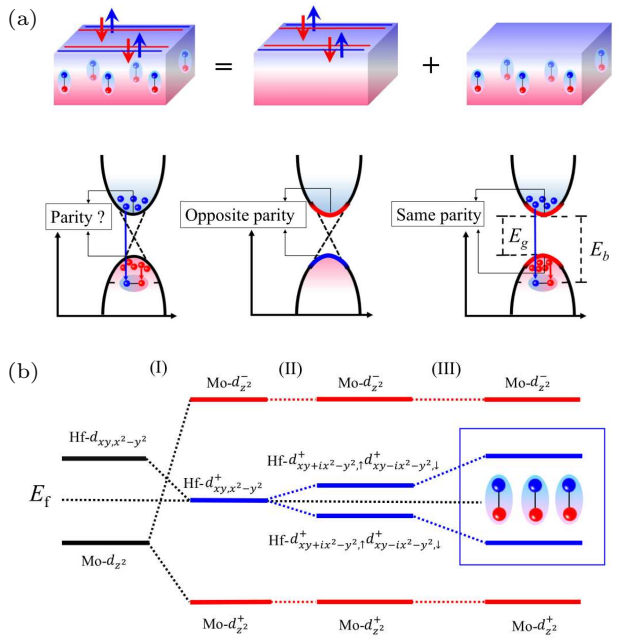


Fig. 4. Schematics of (a) parity frustration in a topological EI and (b) the evolution from atomic orbitals to a topological EI in $Mo_2HfC_2O_2$ at the Γ point. Adapted from Ref. [80].

The above analysis might suggest that intrinsic topological EIs do not exist. In fact, a conventional SOC topological insulator can be understood as the result of two events: (i) the opening of a band gap by SOC, and (ii) state inversions between orbitals of different parity. These two events are often treated together, imposing the additional, sometimes unnecessary, constraint that the band-edge states undergo parity inversion. If parity inversion does not occur at the band edges, a material can still realize a topological EI. Examples include double transition-metal MXenes such as $V_2TiC_2F_2$, $Mo_2TiC_2O_2$, $Mo_2ZrC_2O_2$, and $Mo_2HfC_2O_2$. First-principles BSE calculations confirm that their lowest-energy excitons have negative E_t.[80]

The underlying physics is illustrated in Fig. 4(b) using $Mo_2HfC_2O_2$ as an example. Its electronic structure evolution occurs in three processes. In process (I), the $4d_{z^2}$ orbitals of the two Mo atoms hybridize to form bonding and antibonding states of opposite parity. Here, parity inversion occurs between the reconstructed Mo antibonding state and the Hf 5d state. In process (II), SOC lifts the double degeneracy at the Fermi level, generating a topologically nontrivial gap; in this case, SOC is responsible only for gap opening and does not involve parity inversion. Consequently, the band-edge states derive entirely from Hf 5d orbitals with the same parity. In process (III), electron–hole interactions induce excitonic instability, giving rise to a topological EI.

2.4. Magnetic EIs

It is well known that spontaneous exciton condensation can induce magnetism,[83] but whether excitonic instability occurs in intrinsically magnetic materials remains an open question. Such instability introduces new physics due to the additional spin degrees of freedom. Broadly, excitonic instability in a spin-polarized system can be classified into three cases, as illustrated in Fig. 5(a): (I) Both spins have positive E_t, corresponding to a conventional magnetic semiconductor; (II) Both spins have negative E_t, corresponding to a magnetic EI; (III) One spin has negative E_t while the other has positive E_t, representing a novel state analogous to a half-metal, in which spontaneous exciton condensation occurs in only one spin channel. This state is termed a half-EI.[50]

First-principles BSE calculations identify monolayers of 1T-$NiCl_2$, $NiBr_2$, $CoCl_2$, and $CoBr_2$ as half-EIs.[50] Notably, monolayer $CoCl_2$ has been successfully grown on highly oriented pyrolytic graphite substrates via molecular beam epitaxy,[84] and can alternatively be exfoliated from their layered bulk. Figure 5(b) illustrates the connection between the dark-exciton rule and half-EIs using $NiCl_2$ as an example. The Ni atom resides in a local octahedral environment, where its 3d orbitals split into a threefold t_{2g} and a twofold e_g. Its eight d electrons fully occupy the lower-lying t_{2g} orbitals and the spin-majority channel of the higher-lying e_g orbitals. Consequently, the majority spin features a p–d gap, whose optical transition is dipole-allowed, forming a bright exciton. In contrast, the minority spin features a d–d gap, whose optical transition is dipole-forbidden, forming a dark exciton. The dark-exciton rule thus predicts different excitonic instability behaviors for the two spin channels. First-principles calculations confirm that only the spin-minority E_t is negative (see Fig. 5(c)), while the spin-majority E_t remains positive, resulting in a half-EI.

Remarkably, here the excitonic instability emerges in a wide-gap semiconductor with a single-electron E_g as high as 3.37 eV. This breaks with conventional wisdom that EIs appear in semimetals or narrow-gap semiconductors.[16] Due to

the giant E_b, the ground-state X_1-exciton is very localized and displays a clear Frenkel feature, as reflected in Fig. 5(d). Its formation leads to two neighbouring Ni atoms with different valences, as illustrated in Fig. 5(e), and thus may affect the structural and magnetic properties. For example, unlike the superexchange mechanism within the single-electron picture, the mixed valence of Ni is a hallmark of the double-exchange mechanism. In addition, the spontaneous exciton condensation of a single spin gives its two spins bosonic and fermionic behavior, respectively, and thus very different responses to the external stimulus.

Monolayers of $NiBr_2$, $CoCl_2$, and $CoBr_2$ have similar physics. It is worth mentioning that the E_t of $CoCl_2$ and $CoBr_2$ are as high as -0.59 eV and -0.54 eV, respectively. This implies that excitonic instability may also be present in fewer layers or even in their bulk parents. The main reason for such a large E_t in the Co systems is that their E_g comes from a further splitting of the Co t_{2g} state, and is thus smaller than that of the corresponding Ni compounds.[50]

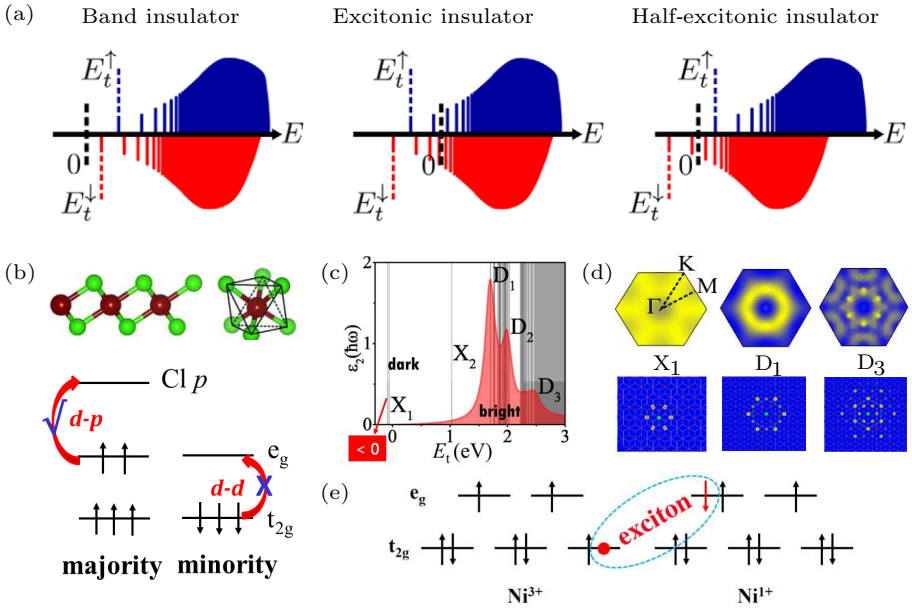


Fig. 5. (a) Schematic representation of three types of excitonic instability in magnetic materials, classified by spin-resolved E_t. When both spins have $E_t > 0$, the system is a normal magnetic insulator; when both have $E_t < 0$, it is a magnetic EI; when one spin has $E_t > 0$ and the other $E_t < 0$, it is a half-EI. (b) Characteristic d-electron configurations in monolayer 1T-$NiCl_2$. (c) Low-energy exciton energies (vertical lines) superimposed on the imaginary part of the BSE dielectric function. X_i and D_i denote dark and bright excitons, respectively. (d) Reciprocal-space (top) and real-space (bottom) exciton wave function moduli. Green dots indicate hole positions fixed at the central Ni atom. (e) Spontaneous formation of X_1 excitons makes neighboring Ni atoms inequivalent, with one behaving like an electron and the other like a hole, as shown in panel (d), exhibiting $+1$ and $+3$ valences, respectively. This mixed valence implies a change in the long-range magnetic interaction from superexchange to double-exchange. Adapted from Ref. [50].

Another special feature of magnetic EI is embodied in the excitonic spin. Traditionally, excitons have always been associated with photoexcitation. Due to conservation of momentum, no spin-flip occurs when an electron is photoexcited. Therefore, only singlet excitons with zero spin are considered (see the left panel of Fig. 6(a)). However, in EIs where excitons form the ground state, the situation is quite different. All that matters now is whether the spontaneous production of excitons lowers the system energy, independent of light. Thus, the spin-selection rule provides another way to realize dark excitons.

Consider a spin-splitting system due to the Zeeman interaction, as shown in the right panel of Fig. 6(a). If an excitonic instability occurs, the electrons and holes that make up this spontaneously generated exciton have the same spin. That is, it is a triplet exciton with spin 1, which leads to a spin-triplet EI.[51] Since the triplet exciton carries spin, once these excitons condense to form a superfluid, a spin superfluidity is developed. The charge neutrality of the excitons prevents their condensation from generating supertransport of charge and thus cannot generate a superconducting-like signal. However, the condensation of triplet excitons can lead to spin superfluidity, providing new opportunities for experimental identification of EIs.

Single-side hydrogenated graphene (graphone) is predicted to be such a spin-triplet EI, as shown in Fig. 6(b).[51] Here, one of the two C p_z-orbitals forms a σ-bond with H, and the unsaturated p_z-orbitals undergo a Zeeman-like splitting, with the electron occupying the lower-lying majority-spin band and emptying the higher-lying minority-spin band. Because the highest valence band and the lowest conduction band are both contributed by the same C atom, the ground-state excitons they form are very localized in real space, extending only about two lattice constants. As a result, the exciton has a giant E_b and exhibits strong bosonic rather than electron–hole pair behavior.

Real-space localization implies reciprocal-space delocalization, which leads to an unexpected indirect-to-direct crossover between single-electron and many-body bands, as plotted in Fig. 6(c). Its single-electron band shows an indirect gap, with the conduction band minimum at Γ and the valence band maximum between Γ and K. However, the calculated exciton band is direct, i.e., the $\boldsymbol{q} = 0$ exciton has the lowest energy. This is virtually impossible in a three-dimensional system and constitutes direct evidence of non-local screening in the low-dimensional system. Since three-dimensional bulk materials have strong screening in all directions, one can simply describe it in terms of a single dielectric constant. The lowest-energy exciton at this point is usually localized only near the top of the valence band and the bottom of the conduction band in reciprocal space. This is quite different in graphone, where the exciton is almost uniformly dispersed throughout the Brillouin zone, and contributions from all k-points must be taken into account. For example, as seen in the inset of Fig. 6(c), in addition to the usual band-extrema transition between ΓQ_1, the Q_2Q_3 transition satisfies the same wavevector requirement; however, the latter corresponds to a single-electron gap of 4.6 eV, which is 1 eV larger than the 3.6 eV of the former.

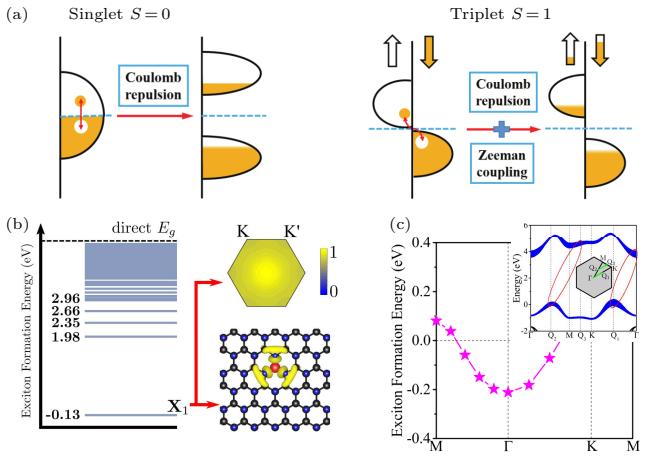


Fig. 6. (a) Comparison of spin-singlet and spin-triplet EIs. When the electron transition occurs within the same spin channel, a singlet exciton with spin 0 is formed. When a Zeeman splitting exists in the system and the electron transitions into the opposite spin, a triplet exciton with spin 1 is formed. (b) First-principles BSE calculations reveal an excitonic instability in graphone, with $E_t = -0.13$ eV for the ground-state X_1-exciton. The exciton is almost uniformly dispersed throughout the Brillouin zone and very localized in real space. (c) Indirect-to-direct characteristic transition between the single-electron band (inset) and the exciton band. The single-electron band exhibits a $Q_1\Gamma$ indirect gap, while the exciton band has its minimum energy at $\boldsymbol{q} = 0$. The inset illustrates the physical essence of non-local screening as the origin of the indirect-to-direct transition. Adapted from Ref. [51].

In Eq. (2), the exchange interaction $V_{vckv'c'k'}$ of the BSE kernel controls the energy splitting between spin-singlet and spin-triplet excitons. Its repulsive nature raises the system energy, and thus the spin-triplet exciton has lower energy. Based on this, spin-triplet EI is also predicted in a semiconducting diatomic kagome lattice, e.g., a superatomic graphene.[54] Therein, the large effective mass of the topologically flat bands drastically reduces the system screening and increases E_b. At the same time, the highly overlapping electron–hole wavefunctions enhance not only the Coulomb direct interaction, but also the exchange interaction, which brings about singlet-triplet splitting up to 0.4 eV.

3. Outlook and perspective

Despite these advances, there are still many key issues to be resolved towards the first recognised EI. This involves the combined efforts and collaboration among the computational, theoretical, and experimental communities, including, but not limited to, searching for and designing suitable candidate materials, developing the theory of excitonic instability and spontaneous condensation, revealing the subtle correlation between spontaneous symmetry breaking and potential superfluidity, and exploring promising applications.

On the computational material design side, there is an urgent need to develop suitable and accurate methods for exciton calculations. Although first-principles BSE is widely used to solve E_g and E_b, it has its limitations. On the one hand, the paradigm can only be applied to semiconductors. For semimetals with small overlap of valence and conduction bands, it remains an open question how to solve for the energetic structure of the exciton. This prevents a direct comparison of E_g and E_b to prove whether a semimetal-EI transition has occurred, e.g., in $TiSe_2$. The key is to develop a method for calculating the dielectric function in the presence of free charge carriers. On the other hand, by its theoretical definition, the EI is ultimately a matter of quantitative comparison between E_g and E_b. However, current first-principles methods cannot accurately predict E_g. Underestimation of E_g is a notorious problem of DFT-based electronic structure methods. Although Hubbard U, hybrid functional and GW can fix it to some extent, these methods are either not well compatible with subsequent BSE or too costly to calculate. It is thus very valuable to solve the E_g problem at the DFT level. Perhaps AI techniques such as deep learning can play a role. For E_b, there is not even enough experience to qualitatively predict the performance of different methods, e.g., whether it is overestimated or underestimated. As a result, different customers may come to completely opposite conclusions because of their different methodological choices. For the same material, some may conclude that it is an EI with $E_t < 0$, while others may conclude that it is a non-EI with $E_t > 0$. Which method, at least statistically, is more reliable is a subject for further research.

On the theoretical side, many-body interactions remain a difficult problem in theoretical physics today. The formulation of BCS theory has greatly advanced the understanding of superconductivity and has also been borrowed to study EIs.

The refinement of the EI theory urgently needs the facilitation of experiments, while on the other hand, experiments lack a powerful means to confirm the EI. This makes the theory and experiment unable to form complementary synergy and fall into the dilemma of "chicken and egg".

While the dark-exciton rule is applicable to almost all known candidates, such as indirect-gap semimetals/semiconductors, quantum-well structures, wide-gap and even strongly-correlated semiconductors, it is neither a sufficient nor a necessary condition for the EI formation. Exploring the instability mechanism originating from optically active bright excitons is not only of fundamentally scientific significance, but also may provide new opportunities for EI identification. As depicted in Fig. 7(a), the excitons in an EI have the same phase due to the macroscopic quantum state nature. Whenever an EI-band insulator phase transition occurs, the excitons become unstable and electrons and holes start to recombine. If the excitons are optically active, the recombination emits coherent light. Such "bright"-exciton EIs can then be identified by their quantum coherence properties. Therefore, although it does not matter whether it is a bright or a dark exciton at the time of the EI formation, there is a difference in the performance during the phase transition. Liu *et al.*[55] propose that an applied transverse electric field can simultaneously drive a band insulator-EI phase transition and activate the dark excitons by breaking the symmetry to realize a bright EI (see the lower two rows of Fig. 3(b)).

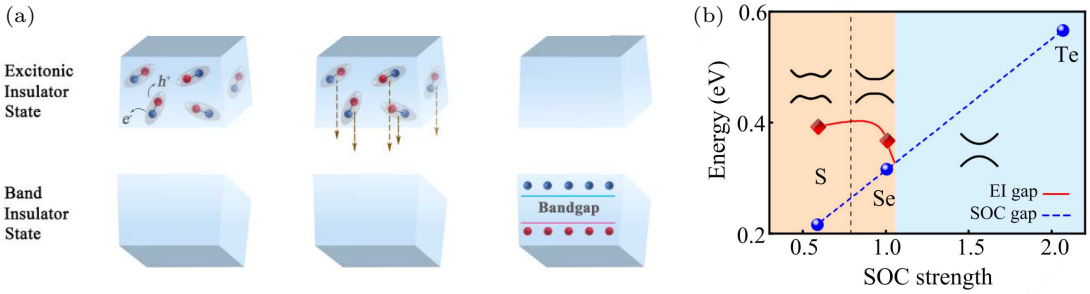


Fig. 7. (a) A schematic diagram of the coherent radiation due to an external field-induced phase transition as a means of distinguishing between a "bright" EI and a band insulator. Adapted from Ref. [55]. (b) Unique bulk–edge correspondence in LiFeX (X = S, Se, and Te) as a means of distinguishing between topological EIs and conventional SOC quantum anomalous Hall insulators. Briefly, since LiFeS and LiFeSe show excitonic instabilities while LiFeTe does not, LiFeSe has the smallest bulk-gap when all have dissipationless topological edge states. If the excitonic instability is not considered, they are all conventional SOC quantum anomalous Hall insulators. The bulk-gap at this point increases linearly from LiFeS to LiFeSe to LiFeTe (blue dashed line). Adapted from Ref. [85].

The lack of "exclusive fingerprints" is arguably one of the most central bottlenecks in the field of EI today. There has been no answer to the question of what unique macroscopic phenomena are translated into by the microscopic mechanism of excitonic instability. At present, identifying an EI is usually done by using abrupt changes induced by exciton condensation reforming band edge states. However, in practice, such macroscopic changes may correspond to more than one microscopic mechanism, and it is difficult to exclude the involvement of all other possibilities. Whether a phenomenological definition of EI can be established, as in the case of superconductors, is at the heart of the matter. In this sense, the combination of EI with topological, magnetic and other orders may open new windows. For example, as shown in Fig. 7(b), a recent study suggests that the unique bulk–edge correspondence serves as an identifying fingerprint for topological EIs.[85] Although this does not ultimately solve the problem of a universal fingerprint for EIs, the interplay between different orderings has the potential to produce unique electrical or optical phenomena, which can be useful to first realize the experimental confirmation of a particular class of EIs.

Acknowledgments

Project supported by the National Key Research and Development Program of China (Grant Nos. 2023YFA1406400 and 2020YFA0308800) and the National Natural Science Foundation of China (Grant No. 12474064).

References

[1] Varsano D, Sorella S, Sangalli D, Barborini M, Corni S, Molinari E and Rontani M 2017 *Nat. Commun.* **8** 1461
[2] Jiang Z, Li Y, Zhang S and Duan W 2018 *Phys. Rev. B* **98** 081408
[3] Kuneš J 2015 *J. Phys.: Condens. Matter* **27** 333201
[4] Huang Y, Shan Y, Du L and Du R 2023 *Acta Phys. Sin.* **72** 177101 (in Chinese)
[5] Wu S, Schoop L, Sodemann I, Moessner R, Cava R and Ong N 2024 *Nature* **635** 301
[6] Kaneko T and Ohta Y 2025 *J. Phys. Soc. Jpn.* **94** 012001
[7] Frenkel J 1931 *Phys. Rev.* **37** 17
[8] Frenkel J 1931 *Phys. Rev.* **37** 1276
[9] Peierls R 1932 *Ann. Physics* **405** 905
[10] Blatt J M, Böer K W and Brandt W 1962 *Phys. Rev.* **126** 1691
[11] Mott N F 1961 *Philos. Mag.* **6** 287
[12] Knox R X 1963 *Solid State Physics* (edited by Seitz F and Turnbull D) Suppl. 5, pp. 100
[13] Keldysh L V and Kopaev Y V 1965 *Sov. Phys.-Solid State* **6** 2219
[14] DesCloizeaux J 1965 *J. Phys. Chem. Solids* **26** 259
[15] Jérome D, Rice T and Kohn W 1967 *Phys. Rev.* **158** 462
[16] Halperin B and Rice T 1968 *Rev. Mod. Phys.* **40** 755
[17] Kohn W and Sherrington D 1970 *Rev. Mod. Phys.* **42** 1

[18] Zittartz J 1968 *Phys. Rev.* **165** 612
[19] Hanamurat E and Haug H 1974 *Solid State Commun.* **15** 1567
[20] Eisenstein J and MacDonald A 2004 *Nature* **432** 691
[21] Mazza G, Rösner M, Windgätter L, Latini S, Hübener H, Millis A J, Rubio A and Georges A 2020 *Phys. Rev. Lett.* **124** 197601
[22] Cercellier H, Monney C, Clerc F, Battaglia C, Despont L, Garnier M G, Beck H, Aebi P, Patthey L, Berger H and Forró L 2007 *Phys. Rev. Lett.* **99** 146403
[23] Kogar A, Rak M S, Vig S, Husain A A, Flicker F, Joe Y, Venema L, MacDougall G J, Chiang T C, Fradkin E, Wezel J V and Abbamonte P 2017 *Science* **358** 1314
[24] Rossnagel K, Kipp L and Skibowski M 2002 *Phys. Rev. B* **65** 235101
[25] Gao Q, Chan Y, Wang Y, Zhang H, Pu J, Cui S, Yang Y, Liu Z, Shen D, Sun Z, Jiang J, Chiang T C and Chen P 2023 *Nat. Commun.* **14** 994
[26] Song Y, Jia C, Xiong H, Wang B, Jiang Z, Huang K, Hwang J, Li Z, Hwang C, Liu Z, Shen D, Sobota J, Kirchmann P, Xue J, Devereaux T, Mo S K, Shen Z X and Tang S 2023 *Nat. Commun.* **14** 1116
[27] Gao Q, Chan Y, Jiao P, Chen H, Yin S, Tangprapha K, Yang Y, Li X, Liu Z, Shen D, Jiang S and Chen P 2024 *Nat. Phys.* **20** 597
[28] Samaneh Ataei S, Varsano D, Molinari E and Rontani M 2021 *Proc. Natl. Acad. Sci. USA* **118** e2010110118
[29] Yang H, Wang X and Li X 2022 *New J. Phys.* **24** 083010
[30] Wakisaka Y, Sudayama T, Takubo K, Mizokawa T, Arita M, Namatame H, Taniguchi M, Katayama N, Nohara M and Takagi H 2009 *Phys. Rev. Lett.* **103** 026402
[31] Windgätter L, Rösner M, Mazza G, Hübener H, Georges A, Millis A J, Latini S and Rubio A 2021 *npj Comput. Mater.* **7** 210
[32] Guo M and Li Y 2024 *Appl. Phys. Lett.* **125** 253105
[33] Huang J, Jiang B, Yao J, *et al.* 2024 *Phys. Rev. X* **14** 011046
[34] Zhang P, Dong Y, Yan D, Jiang B, Yang T, Li J, Guo Z, Huang Y, Haobo Q, Li Y, Kurokawa K, Wang R, Nie Y, Hashimoto M, Lu D, Jiao W H, Shen J, Qian T, Wang Z, Shi Y and Kondo T 2024 *Phys. Rev. X* **14** 011047
[35] Yao J, Sheng H, Zhang R, Pang R, Zhou J, Wu Q, Weng H, Dai X, Fang Z and Wang Z 2024 *Chin. Phys. Lett.* **41** 097101
[36] Jiang B, Yao J, Yan D, Guo Z, Qu G, Deng X, Huang Y, Ding H, Shi Y, Wang Z and Qian T 2024 *Chin. Phys. B* **33** 067402
[37] Hossain M, Cochran T, Jiang Y, *et al.* 2023 arXiv:2312.15862 [cond-mat.str-el]
[38] Wang J, Liu G and Zhang C 2017 *Phys. Rev. B* **95** 075129
[39] Li Z, Nadeem M, Yue Z, Cortie D, Fuhrer M, Wang X 2019 *Nano Lett.* **19** 4960
[40] Wang J, Nie P, Li X, Zuo H, Fauqué B, Zhu Z and Behnia K 2020 *Proc. Natl. Acad. Sci. USA* **117** 30215
[41] Du L, Li X, Lou W, Sullivan G, Chang K, Kono J and Du R 2017 *Nat. Commun.* **8** 1971
[42] Wang R, Sedrakyan T, Wang B, Du L and Du R 2023 *Nature* **619** 57
[43] Liu X, Li J, Watanabe K, Taniguchi T, Hone J, Halperin B, Kim P and Dean C 2022 *Science* **375** 205
[44] Gu J, Ma L, Liu S, Watanabe K, Taniguchi T, Hone J, Shan J and Mak K 2022 *Nat. Phys.* **18** 395
[45] Chen D, Lian Z, Huang X, Su Y, Rashetnia M, Ma L, Yan L, Blei M, Xiang L, Taniguchi T, Watanabe K, Tongay S, Smirnov D, Wang Z Zhang C, Cui Y T and Shi S F 2022 *Nat. Phys.* **18** 1171
[46] Xu Y, Kang K, Watanabe K, Taniguchi T, Mak K and Shan J 2022 *Nat. Nanotechnol.* **17** 934
[47] Tan Q, Rasmita A, Zhang Z, Cai H, Cai X, Dai X, Watanabe K, Taniguchi T, MacDonald A and Gao W 2023 *Nat. Mater.* **22** 605
[48] Lian Z, Meng Y, Ma L, Maity I, Yan L, Wu Q, Huang X, Chen D, Chen X, Chen X, Blei M, Taniguchi T, Watanabe K, Tongay S, Lischner J, Cui Y T and Shi S F 2024 *Nat. Phys.* **20** 34
[49] Wang Z, Rhodes D, Watanabe K, Taniguchi T, Hone J, Shan J and Mak K 2019 *Nature* **574** 76
[50] Jiang Z, Li Y, Duan W. and Zhang S 2019 *Phys. Rev. Lett.* **122** 236402
[51] Jiang Z, Li Y, Zhang S and Duan W 2020 *Phys. Rev. Lett.* **124** 166401
[52] Dong S and Li Y 2020 *Phys. Rev. B* **102** 155119
[53] Dong S and Li Y 2021 *Phys. Rev. B* **104** 085133
[54] Sethi G, Zhou Y, Zhu L, Yang L and Liu F 2021 *Phys. Rev. Lett.* **126** 196403
[55] Liu J, Liu G and Li Y 2021 *Phys. Rev. B* **104** 085150
[56] Liu J and Li Y 2022 *Phys. Rev. B* **106** 035135
[57] Zhao Y, Qu H, Zhao J, Kang L and Zhou S 2025 *Nano Lett.* **25** 1108
[58] Liu J, Qu H and Li Y 2024 *New J. Phys.* **26** 103034
[59] Kasprzak J, Richard M, Kundermann S, Baas A, Jeambrun P, Keeling J, Marchetti F, Szymańska M, André R, Staehli J, Savona V, Littlewood P B, Deveaud B and Dang L S 2006 *Nature* **443** 409
[60] Bucher B, Steiner P and Wachter P 1991 *Phys. Rev. Lett.* **67** 2717
[61] Aryasetiawan F and Gunnarsson O 1998 *Rep. Prog. Phys.* **61** 237
[62] Tan H, Li Y, Zhang S and Duan W 2018 *Phys. Chem. Chem. Phys.* **20** 18844
[63] Tan H, Liu H, Li Y and Duan W and Zhang S 2019 *J. Chem. Phys.* **151** 124703
[64] Marini A, Hogan C, Grüning M and Varsano D 2009 *Comput. Phys. Comm.* **180** 1392
[65] Tiago M, Northrup J and Louie S 2003 *Phys. Rev. B* **67** 115212
[66] Choi J, Cui P, Lan H and Zhang Z 2015 *Phys. Rev. Lett.* **115** 066403
[67] Jiang Z, Liu Z, Li Y and Duan W 2017 *Phys. Rev. Lett.* **118** 266401
[68] Lucking M, Xie W, Choe D, West D, Lu T and Zhang S 2018 *Phys. Rev. Lett.* **120** 086101
[69] Ma M, Han D, Chen N, Wang D and Li X 2022 *Materials* **15** 7715
[70] Sun S, Ren Y, Zhang D, Lou W and Chang K 2024 *Phys. Rev. B* **110** 165430
[71] Qin L, Zhang Z, Jiang Z, Fan K, Zhang W, Tang Q, Xia H, Meng F, Zhang Q, Gu L, West D, Zhang S and Fu Y S 2021 *ACS Nano* **15** 8184
[72] Wang D, Chen Y, Niu Z, Lou W and Chang K 2024 *Chin. Phys. Lett.* **41** 087101
[73] Chen Y, Huang Y, Lou W, Cai Y and Chang K 2020 *Phys. Rev. B* **102** 165413
[74] Agarwal A, Qin Y, Chen B, Blei M, Wu K, Liu L, Shen Y, Wright D, Green M, Zhuang H and Tongay S 2018 *Nanoscale* **10** 15654
[75] Varsano D, Palummo M, Molinari E and Rontani M 2020 *Nat. Nanotechnol.* **15** 367
[76] Jia Y, Wang P, Chiu C, *et al.* 2022 *Nat. Phys.* **18** 87
[77] Sun B, Zhao W, Palomaki T, Fei Z, Runburg E, Malinowski P, Huang X, Cenker J, Cui Y, Chu J, Xu X, Ataei S S, Varsano D, Palummo M, Molinari E, Rontani M and Cobden D H 2022 *Nat. Phys.* **18** 94
[78] Wang R, Erten O, Wang B and Xing D 2019 *Nat. Commun.* **10** 210
[79] Hu L, Zhang R, Zhang F and Wu C 2020 *Phys. Rev. B* **102** 235115
[80] Dong S and Li Y 2023 *Phys. Rev. B* **107** 235147
[81] Yang H, Zeng J, Shao Y, Xu Y, Dai X and Li X 2024 *Phys. Rev. B* **109** 075167
[82] Dong S, Chen Y, Qu H, Lou W and Chang K 2025 *Phys. Rev. Lett.* **134** 066602
[83] Zhitomirsky M, Rice T and Anisimov V 1999 *Nature* **402** 251
[84] Cai M, Miao M, Liang Y, Jiang Z, Liu Z, Zhang W, Liao X, Zhu L, West D, Zhang S and Fu Y S 2023 *Nat. Commun.* **14** 3691
[85] Qu H, Zhang Z and Li Y 2024 arXiv:2412.14600 [cond-mat.str-el]